A comparison of observed and modeled surface waves in southern Lake Michigan and the implications for models of sediment resuspension

Nathan Hawley
Great Lakes Environmental Research Laboratory, Ann Arbor, Michigan, USA

Barry M. Lesht
Argonne National Laboratory, Argonne, Illinois, USA

David J. Schwab
Great Lakes Environmental Research Laboratory, Ann Arbor, Michigan, USA

Received 9 August 2002; revised 21 March 2003; accepted 17 July 2003; published 25 June 2004.

[1] Subsurface pressure sensors were used to make measurements of surface waves during 18 deployments in southern Lake Michigan between 1998 and 2000. Most of the observations were made during the unstratified period (November–May) in water depths between 10 and 55 m. The observations (as well as those obtained from the National Data Buoy Center (NDBC) buoy 45007, which is located in the middle of the southern basin of the lake) were compared to the results obtained from the Great Lakes Environmental Research Laboratory (GLERL)-Donelan wave model implemented on a 2-km grid. The results show that the wave model does a good job of calculating the wave heights, but consistently underestimates the wave periods. In over 80% of the cases the bottom stresses calculated from both the observations and the wave model results agree as to whether or not resuspension occurs, but over 70% of this agreement is for cases when resuspension does not occur; both stresses predict resuspension about 6% of the time. Since the bottom stresses calculated from the model results are usually lower than those calculated from the observations, resuspension estimates based on the wave model parameters are also lower than those calculated from the observed waves. *INDEX TERMS:* 4239 Oceanography: General: Limnology; 4558 Oceanography: Physical: Sediment transport; 4560 Oceanography: Physical: Surface waves and tides (1255); 4594 Oceanography: Physical: Instruments and techniques; *KEYWORDS:* Lake Michigan, wave model, sediment resuspension by waves

Citation: Hawley, N., B. M. Lesht, and D. J. Schwab (2004), A comparison of observed and modeled surface waves in southern Lake Michigan and the implications for models of sediment resuspension, *J. Geophys. Res.*, *109*, C10S03, doi:10.1029/2002JC001592.

1. Introduction

[2] One of the main goals of the Episodic Events Great Lakes Experiment (EEGLE) study (a program funded jointly by NOAA's Coastal Ocean Program and NSF's Coastal Ocean Processes program) is to determine the effects of suspended sediment on the ecosystem in southern Lake Michigan. Accurate models of sediment movement are required to accomplish this goal. Lake-wide numerical models of sediment resuspension and transport have recently been developed and applied to Lake Michigan to simulate resuspension events over wide geographical areas, rather than only at a few specific locations [*Lou et al.*, 2000; *Schwab et al.*, 2000]. Since surface wind waves are the primary cause of sediment resuspension in the lake [*Lesht*, 1989; *Lick et al.*, 1994], modeling of the wave activity is an important component of these models. In the lake-wide models listed above, the GLERL-Donelan wave model [*Schwab et al.*, 1984] was used to calculate the surface wave parameters. This model has been widely used for a number of years to hindcast wave action in both the Great Lakes and other areas [*Lin et al.*, 2002], but while the model is known to accurately calculate the significant wave height and wave direction [*Liu et al.*, 1984; *Schwab and Beletsky*, 1998], it tends to underestimate the wave periods. Since the wave period is important in determining the depth at which sediment suspension occurs, underestimating the period may seriously affect the computation of sediment resuspension in these lake-wide models.

[3] In most previous studies of sediment resuspension in the Great Lakes, direct measurements of surface waves have not been made at the study site(s). This has limited the amount of data available to calibrate the Great Lakes Environmental Research Laboratory (GLERL)-Donelan wave model, and has forced the investigators to either rely

0148-0227/04/2002JC001592$09.00

on wave hindcasts [*Lesht*, 1989; *Lick et al.*, 1994; *Hawley and Lee*, 1999] or to use wave observations made at other locations [*Lesht and Hawley*, 1987; *Hawley et al.*, 1996; *Hawley*, 2000]. In Lake Michigan the GLERL-Donelan wave model has been calibrated and tested using surface wave measurements made at the two NDBC stations (45002 and 45007) located in the center of the northern and southern basins. Since these buoys are retrieved each fall and redeployed each spring, wave conditions during the winter months (when many of the largest storms occur) are not available. The only long-term measurements during the winter months have been made by the Army Corps of Engineers at a station near Gary, Indiana, from 1985–1990 and more recently at a station near Chicago (1991 to present). Although useful, these measurements are available for only these locations and are frequently unavailable during the winter months because of ice cover. In order to better determine the wave heights and periods during large storms, a field program was conducted to measure surface wind waves simultaneously at several sites during the unstratified season. This study reports wave observations made at several locations located around the southern basin of Lake Michigan, compares the wave parameters to those calculated using the GLERL-Donelan wave model, and discusses the implications for models of sediment resuspension in the lake. The focus is on how well the wave model hindcasts agree with the wave observations, so an in-depth analysis of the relationship between surface waves and local resuspension is not included here. A list of the symbols used is given in the notation section.

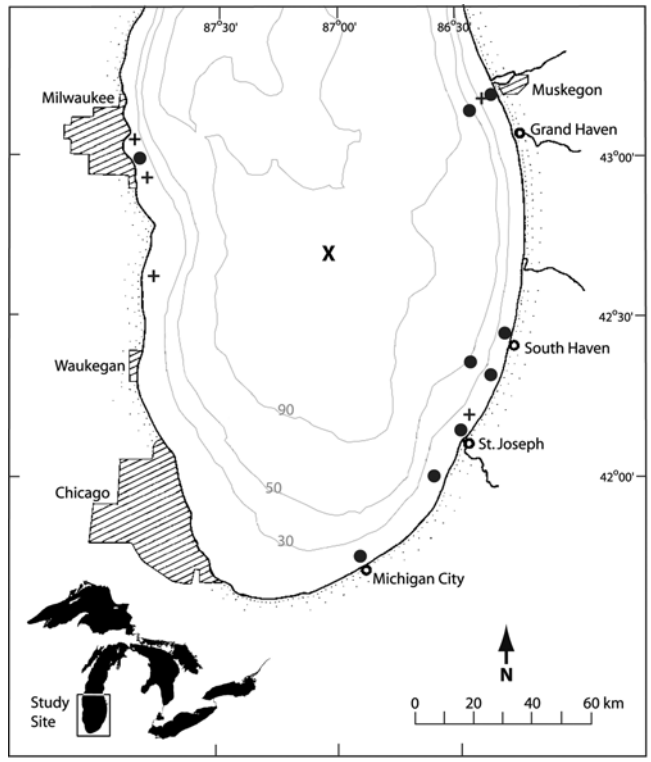

Figure 1. Locations of the moorings and NDBC buoy 45007. The dots are the GLERL moorings, the pluses are the ANL moorings, and the cross is the buoy. Some of the stations were occupied more than once. Depth contours are in meters.

2. Sites and Methods

[4] Moorings were deployed at various times (mostly during the fall and winter) at 18 sites in the southern basin of Lake Michigan between 1998 and 2000 (Figure 1 and Table 1). Moorings are identified by either a mooring number or the name of the nearest town, the last two digits of the year, and the season (sp for spring, su for summer, f for fall, and w for winter). Twelve of the moorings were deployed by GLERL and the other six by Argonne National Laboratory (ANL). Time series measurements of current velocity, water temperature, beam attenuation (a measure of water transparency), and pressure were made at all of the sites, but only the pressure measurements are discussed in this paper.

[5] Paroscientific pressure sensors with a full-scale range of 70 m and an accuracy of 3 mm were used to make all of the pressure measurements. The sensors were attached to a rigid bottom-resting tripod that also supported the data acquisition system. Although the height of the sensors varied from deployment to deployment, they were always located within 1.5 m of the bottom. Differences in the data acquisition systems required that the sampling protocol used for the ANL moorings be different than that used for the GLERL moorings. Pressure observations were made at 4 Hz for 7 min every half hour at the Argonne moorings. The average and standard deviation of the pressure observations made during the first 2 min were computed and stored separately to provide a baseline water depth. All of the sensors were then sampled for another 5 min. The averages and standard deviations of these observations were also computed and recorded, along with the maximum and minimum values, and the covariance between the pressure and both components of the velocity. The average wave period was calculated by subtracting the baseline water depth from the pressure measurement made during the last 5 min, counting the number of zero crossings in the 5-min sample, and then dividing 2 times the sample interval by the number of zero crossings.

[6] Pressure observations at the GLERL moorings were made every half hour except at M15-98su, Benton Harbor-98w, Michigan City-98w, and Milwaukee-98w, when observations were made hourly. All of the observations, which were made at 2 Hz for 2048 samples (except at M15-00f and M55-00f, when observations were made at 4 Hz for 4096 samples), were recorded. The peak-energy wave period was determined by performing a Fourier transform on the pressure measurements after the moorings were retrieved.

[7] The significant wave height at the depth of the pressure sensor was computed using the relationship [*Horikawa*, 1988]

$$4^{*}\sigma_{pr} = H_d. \quad (1)$$

Linear wave theory was then used to calculate the significant wave height at the surface. If the wave period was greater than 15 s, the wave height and wave period were set to zero, since the limited fetch in Lake Michigan makes it unlikely that waves with periods greater than this

Table 1. Mooring Parameters

Station	Latitude	Longitude	Depth, m	Grain Size, mm	Deployed, mm/dd/yy	Retrieved, mm/dd/yy
			ANL Moorings			
Racine-98sp	42°39.90′N	87°44.89′W	15.0		04/02/98	04/30/98
Milwaukee-98su	42°52.22′N	87°42.38′W	25.0		07/23/98	08/24/98
Milwaukee-98f	42°52.17′N	87°42.41′W	25.0		10/28/98	12/01/98
Benton Harbor-99sp	42°12.47′N	86°27.72′W	20.0		04/20/00	06/01/99
Milwaukee-00sp	43°05.65′N	87°50.93′W	20.2		02/28/00	05/16/00
M25-00f	43°12.24′N	86°22.90′W	26.5	0.20	09/13/00	10/31/00
			GLERL Moorings			
M15-98su	43°11.90′N	86°20.03′W	12.0	0.21	07/24/98	08/13/98
Benton Harbor-98w	42°08.09′N	86°29.50′W	10.0	0.56	10/15/98	04/01/99
Michigan City-98w	41°44.11′N	86°54.44′W	11.0	0.21	10/15/98	04/01/99
Milwaukee-98w	42°57.50′N	87°48.79′W	16.1	0.57	10/27/98	05/10/99
M15-98w	43°11.90′N	86°20.03′W	11.0	0.21	11/03/98	11/10/99
South Haven-99f	42°24.23′N	86°19.68′W	18.5	0.31	10/15/99	11/17/99
M04-00sp	41°55.58′N	86°39.92′W	20.8	0.30	03/03/00	05/22/00
M09-00sp	42°14.87′N	86°24.74′W	19.1	0.39	03/03/00	05/22/00
M11-00sp	42°17.36′N	86°30.60′W	40.1	0.05	03/03/00	05/22/00
M15-00sp	43°12.26′N	86°21.15′W	14.8	0.21	04/07/00	05/30/00
M15-00f	43°12.23′N	86°21.32′W	15.9	0.21	09/13/00	10/30/00
M55-00f	43°12.73′N	86°28.65′W	56.5	0.16	09/13/00	11/27/00

would occur. The surface wave parameters determined from both sets of moorings were used as input to determine the bottom shear stress due to wave action (τ) using the method of *Li and Amos* [2001]. This method uses linear wave theory and includes the effects of grain size and bedform geometry when calculating the bottom stress. In addition to the surface wave parameters, this calculation requires that both the water depth and particle size be known. For those stations where we do not have a particle size measurement, we have used a value of 0.35 mm.

[8] The GLERL-Donelan wave model [*Schwab et al.*, 1984] implemented on a 2-km grid was used to calculate the significant wave heights and peak energy periods at hourly intervals. Winds to drive the model at each grid point were determined from an interpolated wind field [*Beletsky and Schwab*, 2001]. The model is parametric and is based on the conservation of momentum applied to deep water waves. The model assumes a Joint North Sea Wave Project (JONSWAP) distribution of wave heights as a function of wave period and is tuned to open water conditions using the observations from the two NDBC buoys (45002 and 45007). The method of *Li and Amos* [2001] was then used to determine the bottom wave stress from the surface wave parameters.

[9] There are several questions that should be considered before a comparison of the observed and modeled wave parameters is attempted: (1) How accurate are the pressure measurements and how large are the errors introduced by using linear wave theory to calculate the surface wave parameters, (2) are the results from the ANL and GLERL moorings compatible, and (3) can the results from the wave model be directly compared to the results from the pressure measurements? These questions are considered below.

[10] Direct measurements of the wave orbital velocity were made during several of the deployments. When these values were compared to the wave orbital velocity calculated from the surface wave parameters derived from the pressure measurements [*Lesht and Hawley*, 2001], the agreement was excellent ($r^2 > 0.9$ in all cases). This agreement confirms the accuracy of both the measurements and the use of linear wave theory to calculate the surface wave parameters from the pressure measurements. Differences in the ANL and GLERL methods to determine the wave height and period at the depth of the pressure sensor were evaluated by using the ANL method on several of the GLERL data sets. Differences between the results were quite minor, although the ANL method occasionally produced waves with a long period (greater than 15 s) and a very low height (less than 1 m). Results from the ANL data sets with these characteristics were removed prior to the analysis.

[11] Because waves with shorter periods attenuate more quickly with depth than do those with longer periods, calculations of the peak-energy period based on subsurface pressure measurements will be biased toward waves with longer periods. This could affect the comparison to the wave periods determined by the wave model, since those periods are for waves at the water's surface. To determine how great this effect is, wave periods calculated by the wave model were recalculated to account for the attenuation with depth using a method suggested by W. Lin and L. P. Sanford (personal communication, 2002). This method assumes a JONSWAP distribution of surface wave energy at the surface, divides the energy into 0.1-s bands between 0.1 and 15 s, uses linear wave theory to determine the energy in each band at the depth of the pressure sensors, and then determines the peak energy period at that depth. Figures 2a and 2b show the significant wave heights and peak energy wave periods calculated by the wave model during two of the deployments, one in 56 m of water (M55-00f) and the other in 10 m of water (BentonHarbor-98w). Both of the data sets show a JONSWAP distribution of wave heights and periods, since the wave model uses the JONSWAP distribution to calculate these parameters from the wind field. After the wave periods have been recalculated, however, the peak energy wave period at 55 m depth is between 8 and 9 s for all but a few very small waves (Figure 2c). The effects are less dramatic in shallower water (Figure 2d), but the recalculated wave periods have a minimum value of about 4 s, and there are some small increases in the longer

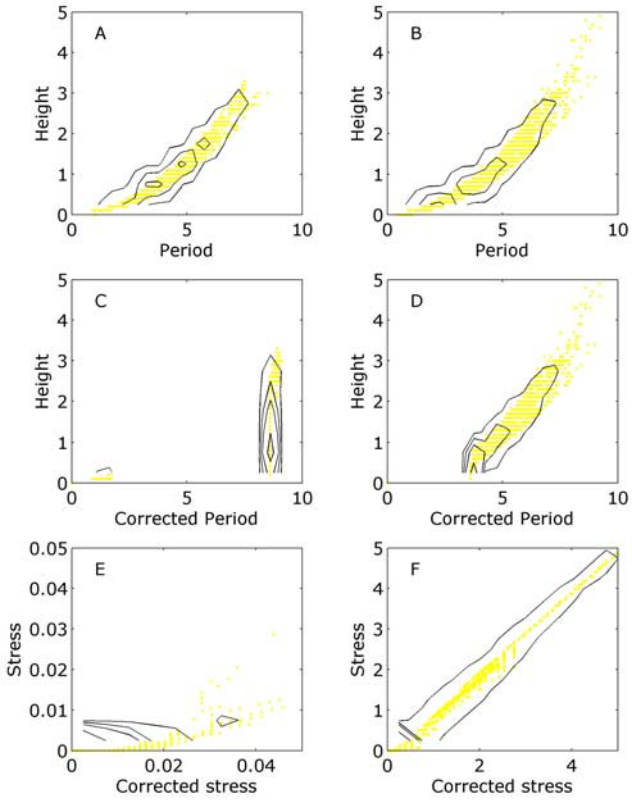

Figure 2. Comparison of the peak energy wave periods calculated by the wave model at two stations. (a, c, e) M55-00f, water depth 56.5 m, 1634 observations. (b, d, f) Station Benton Harbor-98w, water depth 10 m, 4462 observations). The data points are shown in yellow. Data were binned at half-meter and half-second intervals prior to constructing the contours. The contours separate the bins with greater than or fewer than 1%, 5%, 10%, and 25% of the total number of observations. Figures 2a and 2b show the distribution of surface wave peak-energy periods as a function of wave height prior to correcting them to compensate for the attenuation with depth. Figures 2c and 2d show the same comparison after the correction was applied. Figures 2e and 2f compare the bottom stress (in Pascals) calculated with the uncorrected wave periods (*y* axis) and the corrected wave periods (*x* axis). The data in Figures 2e and 2f were grouped at intervals of 0.005 Pascals and 0.5 Pascals. Although the stresses reach values of up to 0.05 Pascals in Figure 2e and 10 Pascals in Figure 2f, over half of the data points in Figure 2e have values less than 0.005 Pascals for both the corrected and uncorrected stress, and over 40% of the points in Figure 2f have values for both stresses less than 0.5 Pascals.

wave periods. The increased wave periods will result in increased bottom stresses, but the increases are relatively small. In shallow water the stresses calculated using the corrected periods are essentially the same as those calculated using the uncorrected periods (Figure 2f), and although in deeper water the stresses computed using the corrected periods are larger than those using the uncorrected periods (Figure 2e), the values are quite small in both cases. In order to be consistent, however, all of the wave model periods were recalculated prior to comparing them to the periods calculated from the pressure observations.

3. Results

3.1. Surface Wave Parameters

[12] Hourly observations of the significant wave height and peak energy wave period are made at NDBC buoy 45007 (deployed in the center of the southern basin of Lake Michigan at 42°40.2′N, 87°01.2′W, water depth 165 m) each year from mid-March through early December. The significant wave heights and peak energy wave periods calculated from the wave spectra data measured at the buoy in 1998–2000 are compared to the results of the wave model in Figure 3. Maximum values of the observed and

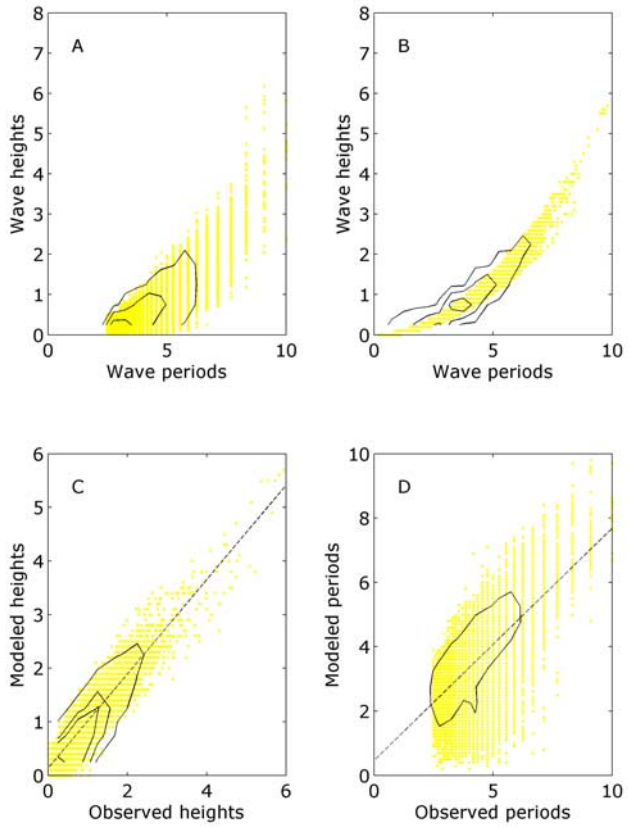

Figure 3. Observed and modeled surface wave parameters from NDBC station 45007 for 1998–2000. The 16,198 data points are in yellow. Data were binned at half-meter and half-second intervals prior to constructing the contours. The contours separate the bins with more or less than 1%, 5%, 10%, and 25% of the total number of observations. (a) Observed significant wave height and peak energy wave period. About 44% of the data points have heights less than 0.5 m. (b) Modeled significant wave height and peak energy wave period. About 33% of the data points have wave heights less than 0.5 m. (c) Observed and modeled wave heights. The dashed line is the regression line listed in Table 2. About 30% of the data points have both an observed and modeled height less than 0.5 m. (d) Observed and modeled wave periods. The dashed line is the regression line listed in Table 2. There is no significant concentration of the data points at a particular value.

Table 2. Comparison of Observed and Modeled Wave Heights and Periods[a]

	Buoy 45005	GLERL Tower	Buoy 45007	Pressure Data, All Observations	Pressure Data, Non-Zero Observations
Number of observations	1423	890	16,198	30,126	14,248
Height range	0–2.5 m	0–3 m	0–6 m	0–8 m	0–8 m
Intercept	0.03 m	−0.002 m	0.13 m	0.40 m	0.25 m
Slope of line	0.68	0.99	0.88	0.64	0.71
R^2	0.77	0.86	0.88	0.63	0.69
Period range	1–6.5 s	2–7 s	2–10 s	0–15 s	0–15s
Intercept	0.52 s	0.09 s	0.47 s	4.91 s	1.94 s
Slope of line	0.69	0.77	0.72	0.04	0.50
R^2	0.52	0.66	0.46	0.01	0.40
Stress range			0–10 Pascals	0–15 Pascals	0–15 Pascals
Intercept			−0.11	0.86	0.47
Slope of line			0.70	0.74	0.75
R^2			0.71	0.69	0.63

[a]The coefficients and fit of a linear regression of the modeled and observed parameters are given for the significant wave height, peak-energy wave period, and bottom shear stress. The first two columns are the results of *Schwab et al.* [1984]; stress calculations were not done for these data sets. The last two columns are the results from the pressure observations with and without the observations when no wave motion was observed by the pressure sensor.

modeled wave heights and periods are about the same, but there are several differences between the observed parameters and those calculated by the wave model. The most noticeable is that the observations show considerably more variability in the distribution of wave heights as a function of wave period than do the model results, which are calculated using the JONSWAP relation. One limitation of the buoy observations is that wave periods less than 2.5 s are reported as 0 s; these data have been removed from both the observed and wave model results. However, there are still many times when the wave model calculates a period less than 2.5 s. The observations have a large concentration of data points with wave heights less than 0.5 m (44%), while the wave model results have wave heights less than 0.5 m only 33% of the time and show a concentration of heights between 0.5 and 1.0 m. In spite of these differences, a linear regression of the observed and modeled heights shows that the model calculates the heights quite well (Table 2), but the agreement is not as good for the periods. In most cases the model calculates a wave period smaller than that observed, but in some cases the reverse is true. The observed periods are not always small during these instances, so the differences are not always due to the failure of the buoy to record small waves. Table 2 shows that the comparisons presented here are quite similar to the results from the two data sets presented by *Schwab et al.* [1984].

[13] The accuracy of the buoy observations should be considered when comparing the wave model parameters to the observed ones. If one sets upper and lower error bounds around H_o and P_o equal to the accuracy of the measurements (0.2 m and 0.01 s^{-1}), then one can determine what percentage of the wave model parameters (H_m and P_m) fall within those bounds. These results (Table 3) show that H_m falls within the error bounds approximately 70% of the time, with the remainder of the observations distributed about 2:1 between occurrences where H_m exceeds H_{ub} and occurrences where H_m is less than H_{lb}. The average difference between H_o and H_m is less than 0.5 m in all cases. The differences between P_o and P_m are much more pronounced. P_m is less than P_{lb} about 70% of the time, with an average difference of over 1 s. Only about 15% of the model periods fall within the error bounds, while the other 15% exceed P_{ub}. Instances when both model parameters fall within the error bounds occur only a small percentage of the time (10%).

[14] Most of the pressure measurements were made between October and April, but many of the buoy observations were made between May–September. To determine whether or not the summer observations (when the waves are smaller) biased the results, all of the buoy observations made during May–September were removed and the analysis redone. The results are slightly different (Table 3), but the general pattern is the same as that obtained for all of the observations. The wave model does a slightly better job of predicting the periods if the summer observations are removed, but the difference is not great.

[15] The wave parameters determined from the pressure observations and the corresponding wave model results are shown in Figure 4. These observations show some waves considerably larger than those observed at the buoy; wave heights ranged up to 8 m and wave periods to 15 s. The observations also show an even broader range of wave

Table 3. Comparison of the Surface Wave Parameters From the Buoy Observations to Those From the Wave Model[a]

	N45007 Data	N45007 Non-Summer	Pressure Stations
Number of observations	16,198	7244	14,248
$H_m > H_{ub}$	18.7%	22.3%	26.4%
H_m-H_o	0.3 m	0.3 m	0.5 m
$H_{lb} <= H_m <= H_{ub}$	70.5%	65.4%	39.4%
H_m-H_o	0.0 m	0.0 m	0.0 m
$H_m < H_{lb}$	10.8%	12.3%	34.2%
H_m-H_o	−0.4 m	−0.4 m	−0.6 m
$P_m > P_{ub}$	14.2%	17.0%	4.4%
P_m-P_o	0.5 s	0.5 s	0.6 s
$P_{lb} <= P_m <= P_{ub}$	15.6%	20.0%	15.6%
P_m-P_o	0.0 s	0.0 s	−0.1 s
$P_m < P_{lb}$	70.1%	63.0%	80.0%
P_m-P_o	−1.2 s	−1.2 s	−1.5 s
$H_{lb} <= H_m <= H_{ub}$ and $P_{lb} <= P_m <= P_{ub}$	10.6%	13.5%	5.8%
H_m-H_o	0.1 m	0.1 m	0.0 m
P_m-P_o	0.0 s	0.0 s	−0.1 s

[a]Non-summer data means that the observations from May–September were excluded. The percentages are the occurrences of the criterion given in the left-hand column. Mean differences between the modeled and observed parameters are also given.

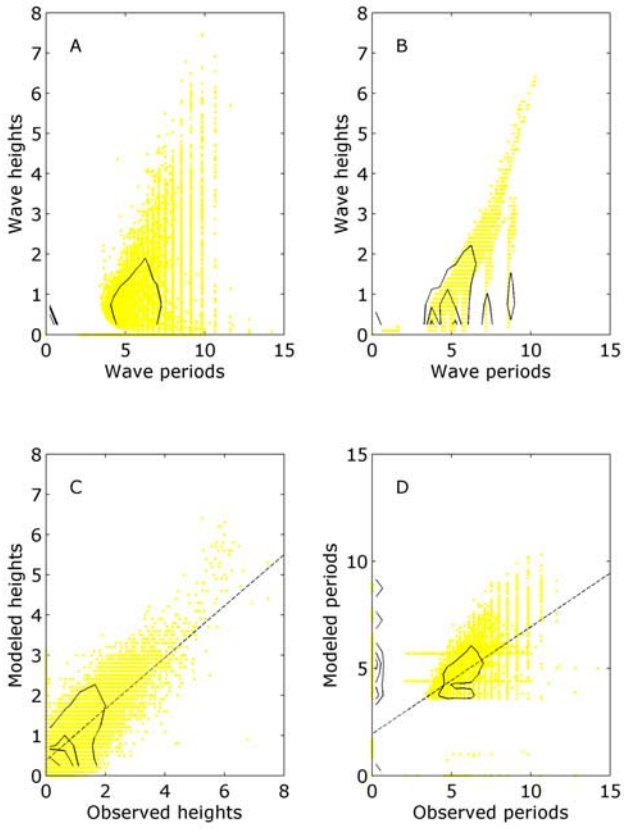

Figure 4. Observed and modeled wave parameters from the pressure observations. The 30,126 data points are in yellow. Data were binned at half-meter and half-second intervals prior to constructing the contours. The contours separate the bins with more or less than 1%, 5%, 10%, and 25% of the total number of observations. (a) Observed significant wave height and peak energy wave period. No wave motion was observed in over half of the observations. (b) Modeled significant wave height and peak energy wave period. Over 35% of the data points have a wave height less than 0.5 m. (c) Observed and modeled wave heights. The dashed line is the regression line listed in Table 2. Over 75% of the data points have both observed and modeled heights less than 0.5 m. (d) Observed and modeled wave periods. Over half of the data points have P_o equal to zero. The dashed line is the regression line using only the data when P_o is greater than zero (14,248 observations).

heights at a given period than do the buoy observations. However, in over 50% of the observations, no wave motion was observed, so both H_o and P_o are equal to zero. The results from the wave model (Figure 4b) deviate from the JONSWAP distribution shown in Figure 3b because of the recalculation of the wave periods to account for the attenuation of the shorter waves with depth. Thus both the observed and modeled wave periods in Figure 4 are the peak energy wave period at the depth of the sensor, not the peak energy wave period at the surface.

[16] The heights from the wave model agree fairly well with the observations (Table 2, although not as well as for the buoy observations), but the wave model periods are consistently lower than those observed. The poor results of the linear regression between the observed and modeled periods is due in large part to the large number of observations (over 50%) when no waves were observed by the pressure sensors but for which the wave model calculated a non-zero wave period. These occurrences are also included in the comparison of the heights, but because the modeled heights are close to zero, they are not as noticeable. If these observations are removed, then the regression for the wave periods gives a more realistic value for the modeled wave period although the fit is still not very good. This is the regression line shown in Figure 4d.

[17] Although the accuracy of the pressure measurements is 3 mm, it is difficult to determine what the errors are for the wave parameters calculated from these measurements. For consistency, the upper and lower bounds for the surface wave parameters were calculated using the same values as for the buoy observations. The value of 0.01 s^{-1} for the wave frequency is greater than the resolution of the Fourier transform for all but the longest wave periods. The results show (Table 3; note that the observations where the observed wave period equals zero have been removed since upper and lower bounds cannot be calculated) that the percentage of model wave heights that fall between the upper and lower bounds is about 25% less than the percentage for the buoy observations, while the percentage less than the lower bound increases by about the same amount. An even higher percentage (80%) of the modeled wave periods are less than the lower bound of the observed periods, while only 4% exceed the upper bound. The mean differences between the wave parameters derived from the wave model and those calculated from the observations are also slightly larger than the differences based on the buoy observations, and in less than 6% of the observations do both H_m and P_m fall within the error bounds. Thus the agreement between the observed and modeled wave parameters based on the pressure data is much poorer than for the surface observations.

3.2. Bottom Stress

[18] To determine what effect the differences between the observed and modeled wave parameters have on sediment resuspension, it is necessary to calculate the stress exerted by the waves on the lake floor. The stresses calculated from the observations (τ_o) and from the wave model results at the buoy (τ_m) were calculated for a range of depths (10–50 m) and grain sizes (0.1–0.5 mm). The results for a depth of 20 m and a grain size of 0.35 mm (these are the average depth and particle size for all of the pressure observations) are shown in Figure 5a. Although there is some correlation between τ_m and τ_o, the scatter is considerable. For particles this size the method of *Li and Amos* [2001] gives a critical stress for resuspension of 1.36 Pascals (τ_b; the stress required for bed load movement is 0.24 Pascals), so in many cases, both estimates of the stress predict resuspension even though the actual values may differ considerably. Table 4 compares the frequencies with which no movement, bed load, and resuspension are predicted by τ_o and τ_m. The results show that 84.5% of the time τ_m and τ_o agree as to whether no transport, bed load transport, or resuspension will occur. The two stresses both predict that resuspension will occur 5.9% of the time, but there are just as many instances in which only one of the two stresses predict

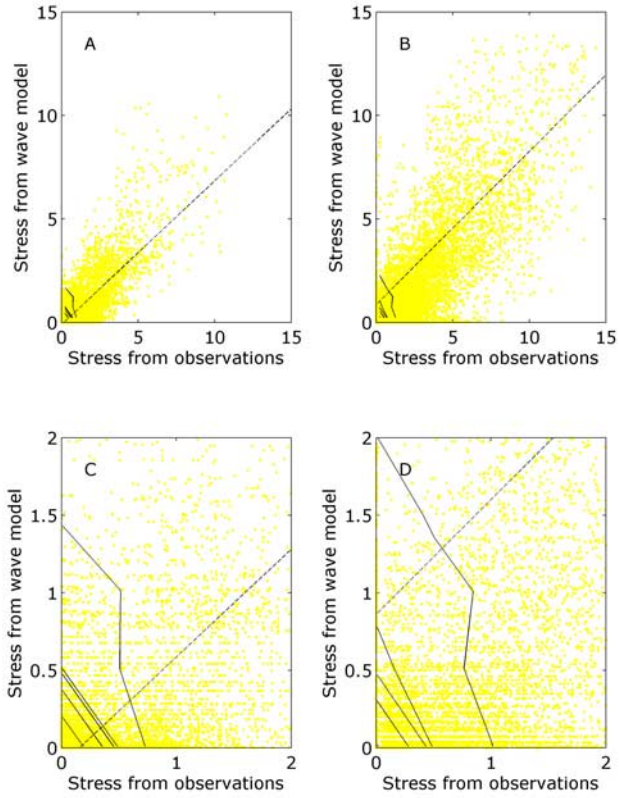

Figure 5. Bottom stresses (in Pascals) calculated from the observations and from the wave model results at (a, c) buoy 45007 (16,128 observations) and (b, d) the 18 pressure moorings (30,126 observations). The data points are shown in yellow. Data were grouped at intervals of 0.5 Pascals prior to drawing the contours. The contours separate the bins that greater than or fewer than 1%, 5%, 10%, and 25% of the total number of observations. Figures 5c and 5d show the details of the observations in the lower left corner of Figures 5a and 5c. The dashed lines are the linear regressions with τ_o as the independent variable and τ_m as the dependent variable. In Figures 5a and 5c, over 75% of the data points have values less than 0.5 Pascals for both τ_o and τ_m. In Figures 5b and 5d, about 25% of the data points have values less than 0.5 Pascals for both τ_o and τ_m.

resuspension; in these cases the average difference between the two stresses can increase to over 1.7 Pascals (as compared to an average difference of 0.5 Pascals when both stresses predict resuspension).

[19] The frequencies in Table 4 can be used to construct a skill score [*Panofsky and Brier*, 1968] to determine how well the predictions of transport using τ_m agree with the predictions using τ_o. *Lesht* [1989] used this technique to quantify predictions of sediment transport on the Indiana shoals. The resulting skill score (0.55) is significantly different from zero at the 95% confidence level (based on a χ^2 distribution with 4 degrees of freedom), so the results using τ_m are significantly better than chance at predicting the type of transport. A contingency table for the buoy data with the summer months removed gives similar results (skill score of 0.62). Comparisons of τ_o and τ_m calculated using other depths and particle sizes also give similar skill scores, although of course the occurrence of resuspension events increases with both decreasing depth and decreasing particle size.

[20] A comparison of the stresses calculated from the pressure measurements to those calculated from the wave model results (Figure 5b) shows even more scatter than for the buoy data. Table 5 shows the contingency table for these stresses. The two stresses agree 75.2% of the time as to whether no transport, bed load transport, or suspension will occur, but most of the agreement occurs when both stresses predict no movement. The average difference between τ_o and τ_m when both predict suspension is 0.4 Pascals, but this difference increases to 0.9 Pascals if only τ_o predicts suspension and to over 0.8 Pascals if only τ_m predicts suspension. The skill score for the data in Table 3 is 0.55, so τ_m does a significantly better job of predicting the mode of transport than would be obtained by chance. Skill scores determined for each of the individual moorings ranged between 0 and 0.72, but in most cases at least one of the entries in the contingency table was zero. Since this invalidates one of the conditions required for use of the χ^2 distribution as a test for goodness of fit, the significance of the scores for the individual deployments cannot be evaluated. As should be expected, the frequency with which resuspension is predicted is higher when the pressure observations are used (since the buoy observations include the summer data), but in both cases the wave model does an excellent job of predicting the correct type of particle movement.

4. Discussion

4.1. Surface Wave Parameters

[21] The agreement between the modeled wave parameters and the buoy observations (Table 2) is consistent with the results presented by *Schwab et al.* [1984] even though

Table 4. Bottom Stresses in Pascals Computed From Buoy 45007 Observations (τ_o) and From Wave Model Parameters (τ_m)[a]

	Observed Stresses			
Model Stresses	$\tau_o >= \tau_r$	$\tau_r > \tau_o >= \tau_b$	$\tau_b > \tau_o$	Total
$\tau_m >= \tau_r$	946, 5.9% $\tau_o - \tau_m = 0.59$	143, 0.9% $\tau_o - \tau_m = -0.85$	19, 0.1% $\tau_o - \tau_m = -1.74$	1108
$\tau_r > \tau_m >= \tau_b$	636, 3.9% $\tau_o - \tau_m = 1.40$	942, 5.8% $\tau_o - \tau_m = 0.16$	423, 2.6% $\tau_o - \tau_m = -0.44$	2001
$\tau_b > \tau_m$	165, 1.0% $\tau_o - \tau_m = 1.72$	1397, 8.6% $\tau_o - \tau_m = 0.56$	11969,73.7% $\tau_o - \tau_m = 0.09$	13089
Total	1747	2482	11969	16198

[a]Computations were done for a water depth of 20 m and a particle size of 0.35 mm. The number of observations, the percentage of the total observations, and the mean difference between the two stress estimates are given in each cell.

Table 5. Bottom Stresses in Pascals Computed From All of the Pressure Observations (τ_o) and From Wave Model Parameters (τ_m)[a]

	Observed Stresses			
Model Stresses	$\tau_o >= \tau_r$	$\tau_r > \tau_o >= \tau_b$	$\tau_b > \tau_o$	Total
$\tau_m > = \tau_r$	4425,14.7% $\tau_o - \tau_m = 0.67$	558, 1.9% $\tau_o - \tau_m = -1.58$	780, 2.6% $\tau_o - \tau_m = -0.93$	5763
$\tau_r > \tau_m >= \tau_b$	1092, 3.6% $\tau_o - \tau_m = 1.91$	3012,10.0% $\tau_o - \tau_m = 0.26$	1989, 6.6% $\tau_o - \tau_m = -0.47$	6093
$\tau_b > \tau_m$	1098, 3.6% $\tau_o - \tau_m = 1.51$	1967, 6.5% $\tau_o - \tau_m = 0.70$	15205,50.5% $\tau_o - \tau_m = -0.04$	18270
Total	6615	5537	17974	30126

[a]Water depths and particle sizes for the different moorings are given in Table 1. The number of observations, the percentage of the total observations, and the mean difference between the two stress estimates are given in each cell.

the data set presented here is considerably larger and includes waves with much greater heights and longer periods. This indicates that Schwab et al.'s results are robust and that the wave model can be used with some confidence to predict surface wave parameters, in particular the significant wave height. However, it is important to realize that the wave model was tuned to fit the data from the buoy, so the results presented here are the best possible model results. The agreement between the wave parameters derived from the pressure measurements and the wave model parameters is not as good. Since the pressure measurements are the more appropriate data to use when considering how well the wave model will predict bottom resuspension, comparisons of the model results to surface measurements may present too optimistic an assessment of the wave model's ability to predict resuspension events.

[22] Although the wave model does not do a particularly good job of predicting the wave periods, other models will probably do no better. *Lin et al.* [1997] compared the results from five different wave models to observations made in the Chesapeake Bay and found that the GLERL-Donelan wave model did at least as well as the other models. There are several possible reasons for the failure of the model to accurately predict the wave periods: The deep water formulation of the model may be inapplicable to the observations (the non-zero pressure observations are by definition made in intermediate or shallow water), the JONSWAP relation may not accurately describe the waves in the lake, the propagation of waves with time from the area where they are generated may be wrong, or the over-lake wind field (which is derived from interpolation of the wind field measured at various point around the lake) may not be accurate enough. It may also be (as suggested by *Liu et al.* [2002]) that the characterization of the wave field by an energy spectrum may not be an adequate description of the wave characteristics. Given the accuracy of the model in predicting the wave heights, it seems unlikely that the JONSWAP formulation is seriously in error or that shallow water effects are significant, but the relative contributions of the other possible errors are difficult to quantify. It may be that local variations in wind conditions are the single most important source of error, but without over-lake wind measurements at numerous sites, it is impossible to assess its importance.

4.2. Bottom Stress

[23] The agreement between τ_o and τ_m in predicting the type of transport is somewhat surprising given the disparity between the estimates of τ_o and τ_m (Figure 5). Part of the agreement is because both bed load and suspension can occur over a wide range of stresses. The critical stresses required for bed load movement and for suspension are both functions of the particle size (Figure 6), but the critical stress required for bed load movement increases only slightly as the particle size increases and does not exceed 0.5 Pascals for the range of particle sizes found at the moorings. Since the critical stress required for suspension increases much more rapidly with particle size, bed load will occur over a wider range of stresses for larger particles than for smaller ones. Since suspension will occur whenever the stress exceeds the critical value, suspension can also occur over a wide range of stresses regardless of particle size. This does not, however, explain the good agreement between τ_o and τ_m in predicting no movement, which

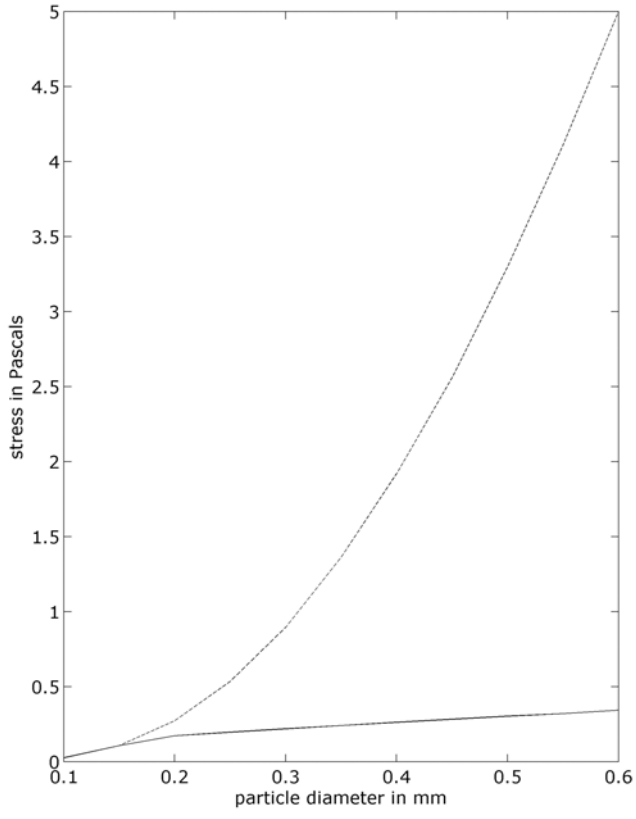

Figure 6. Critical stress (in Pascals) required for bed load movement (solid line) and sediment resuspension (dashed line) as a function of particle size (diameter in millimeters) calculated using the method of *Li and Amos* [2001].

accounts for over 50% of the observations. This agreement appears to be due partly to the wave climate of the lake, in which there are extended periods when only small or no waves exist, and partly to the model's ability to accurately calculate the parameters for these smaller waves. In only 2.7% of the data does τ_m predict movement when none is predicted by τ_o, while in another 9.6% of the data, τ_m fails to predict movement when τ_o does (Table 5).

4.3. Prediction of Resuspension Rate

[24] Although the agreement between τ_o and τ_m in predicting the type of transport is quite good, there are often substantial differences in the actual values of the two stresses (Table 5). These differences may be important when trying to calculate the rate of suspension of the bed material. One commonly used model of the rate of suspension is a power law formula (see *Sanford and Maa* [2001] for an extensive discussion of erosion formulas),

$$E = M(\tau - \tau_r)^n. \quad (2)$$

The form of equation (2) makes the amount of resuspended material linearly dependent on the excess stress $(\tau - \tau_r)$ when n equals 1 (n is usually between 1 and 5). In theory, errors in τ can be partially compensated for by adjusting the value of M, but this works only in an average sense unless the difference between the two is relatively constant over time. If n is not equal to 1, then the dependence becomes nonlinear, and it is much more difficult to compensate for errors in τ_b.

[25] A detailed analysis of all of the data collected is beyond the scope of this investigation, but examination of the time series of the bottom stresses shows that the differences between τ_o and τ_m are certainly not constant over time. This is shown in the values given in Table 5, which show that the differences between τ_o and τ_m when both are less than τ_r are considerably less (0.04–0.70 Pascals) than when at least one of them is greater than τ_r (0.67–1.91 Pascals). Figure 7 shows the wave parameters calculated from the pressure measurements and by the wave model for a segment of the data recorded at Michigan City during the fall of 1998. The agreement between the wave heights is quite good, but there are numerous instances when P_m is considerably less than P_o. The figure also shows that there are a large number of times when no waves were recorded by the pressure sensor, and that most of the occurrences when the bottom stress exceeds τ_r occur during distinct events separated by times when the stress is low. During these events the stress first increases quickly then decays more slowly as the storm wanes. The most frequently observed pattern in these cases is that the maximum τ_o exceeds the maximum τ_m and that the difference between the two then decreases with time. However, in some cases, τ_m exceeds τ_o (for instance, on day 315). The periods at the end of the storms account for the bulk of the occurrences when either τ_o or τ_m, but not both, exceed τ_r, but there are some instances (not shown) when either the wave model falsely predicts a resuspension event or the wave model completely misses an event recorded by the pressure sensors.

[26] The variability in the difference between τ_o and τ_m (Figure 7d) makes it extremely difficult to correct for errors in τ_m by adjusting the value of τ_r (or M) in equation (2). The mean difference for the data shown in Figure 7, for example,

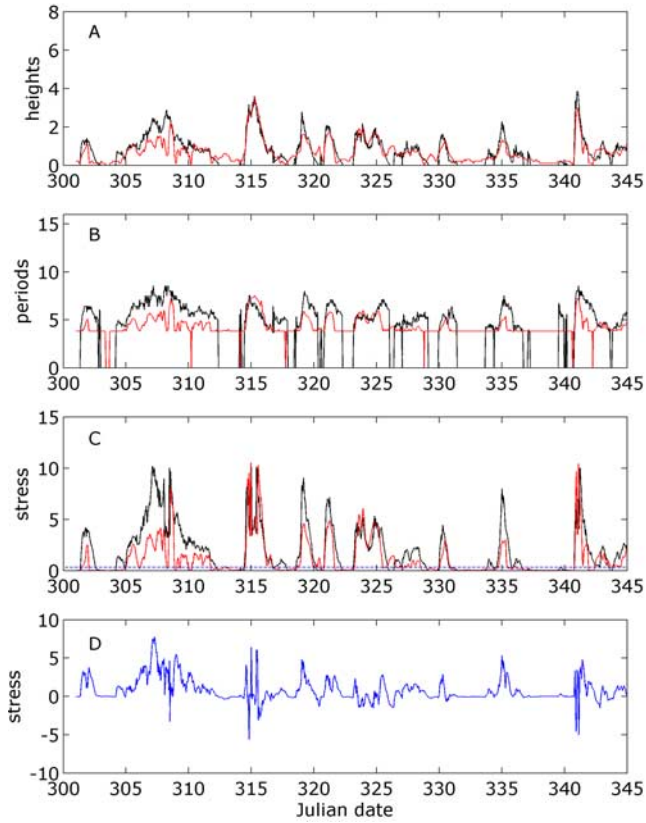

Figure 7. Data from Michigan City during the fall of 1998. (a) Observed (black line) and model (red line) significant wave heights (m), (b) observed (black line) and model (red line) peak energy wave periods, and (c) bottom stress (Pascals) calculated from the observations (black line) and from the wave model results (red line). The dashed blue line is the stress required for resuspension at this location. (d) The difference between the stress calculated from the observations and that calculated from the model.

is 0.72 Pascals, but adding this to τ_m would not increase the values sufficiently during times when τ_m is high, but would increase them enough to falsely indicate resuspension during intervals when τ_o does not. The variability in the difference between τ_o and τ_m is reflected in the standard deviation of the difference between τ_o and τ_m (1.17 Pascals for all of the observations in Table 5), which is considerably higher than the mean difference (0.19 Pascals). This difference is in part due to the variation in depth and grain size at the different stations, but even at a single station the standard deviation of the difference is greater than the mean difference.

4.4. Comparison to Other Sources of Error in Resuspension Models

[27] Given the possible errors in predicting resuspension rates based on results from the wave model, and the difficulty in compensating for these errors, it is important to examine how important these errors are compared to other errors in resuspension models. Two different cases can be considered. The first is when results are desired at only a few specific sites, and the second is when the results over a wide area are needed. In both cases an accurate determination of the stress required to suspend the bottom material is needed,

but the value of this stress depends upon the properties of the sediment as well as on the water depth and the size of the waves. For noncohesive material (particles larger than about 60 μm) the particle size and density are generally considered to be sufficient to predict the stress required for resuspension, but for cohesive sediments, other factors, including chemical and mineralogic composition, depositional history, and the extent of biological reworking also need to be considered. If only a few sites are involved, then it may be possible to specify both the water depth and the bed properties with some degree of accuracy based on actual measurements, so the value of τ_r (and the particle settling velocity, which is also dependent upon particle size) can be determined independently of the time series measurements. This should constrain the possible values of the other variables in the model and allow the effects of using the wave model to be identified. In an exploratory analysis, *Lesht and Hawley* [2001] applied a simple resuspension model to the data collected at station M2500f, and found that the major features of the turbidity record could be simulated using either τ_o or τ_m as the forcing function. However, they did not include the actual particle size in their analysis, nor did they investigate in any detail the differences in the results using the two sets of stress estimates. Further analysis of the data sets presented here (in conjunction with time series measurements of turbidity and current velocity) should allow the possible errors introduced by using the wave model results to be better characterized.

[28] In the second case, neither the water depth nor the bed properties are likely to be particularly well specified. The lake-wide circulation model for Lake Michigan, for instance, has been implemented on a 2-km grid [*Schwab et al.*, 2000], so a single depth has to be assigned to each grid cell, even though the depth within a cell may vary by 10 or more meters. Although the stress required for resuspension is very dependent upon the properties of the sediment, for the vast majority of the over 14,000 grid boxes in the 2-km Lake Michigan model, little sediment information is available. This means that an estimate of the sediment properties must be extrapolated from the relatively few measurements that are available, so in most cases an estimate of the stress required to erode the material is little more than guesswork. This may not be too important in the deeper areas of the lake (where resuspension is unlikely and the particles can be safely considered to be fine-grained material), but in the areas where resuspension is likely to occur (in water depths up to 50–80 m), a knowledge of the sediment properties is critical. Unfortunately there are few systematic studies of bottom properties in Lake Michigan. The most comprehensive is that reported by *Cahill* [1981], but even in this survey, there are relatively few measurements made compared to the number of grid boxes (Cahill's samples were collected on a 12-km grid). Given the assumptions that must be made about bed properties and water depth, it seems likely that the errors introduced by using the wave model results are relatively small.

5. Conclusions

[29] Time series measurements of subsurface wave action were made at 18 different locations in southern Lake Michigan (mostly between October and May) between 1998 and 2000. The surface wave parameters derived from these measurements differ considerably from the wave parameters calculated by the GLERL-Donelan wave model. The agreement between the wave parameters determined from surface measurements and those calculated by the wave model are somewhat better, and are similar to results published previously. This study confirms previous work that shows that although the wave model accurately predicts the wave height, it frequently underpredicts the wave period.

[30] The bottom stresses calculated from the wave model results are usually less than those derived from the pressure observations, and there is considerable scatter in the results. However, in over 80% of the cases, the two estimates agree as to whether or not resuspension or bed load movement will occur. The majority of this agreement, however, (over 70%) occurs when both estimates predict no motion. Both estimates predict resuspension in about 6% of the cases.

[31] Since the estimates of the bottom stress calculated from the model results are usually lower than those calculated from the observations, estimates of the rate of sediment suspension will also be low, since the rate of suspension is dependent upon the excess stress (the amount the bottom stress exceeds that required for suspension). The difference between the observed and modeled stresses varies considerably with time, which makes it difficult to correct for the errors introduced by using the wave model. However, given the lack of knowledge of the distribution of properties in Lake Michigan, the errors introduced by using the wave model are likely to be relatively small when modeling large-scale phenomena. When site-specific results are desired the errors may be more important, but further analysis is required before the importance of these errors can be quantified.

Notation

E	rate of erosion, g/m^2/s.
H_d	significant wave height at depth d, m.
H_o	significant wave height based on the observations, m.
H_m	significant wave height based on the wave model results, m.
H_{lb}	lower bound of H_o, m.
H_{ub}	upper bound of H_o, m.
M	an empirical constant, s/m.
N	an empirical constant, no units.
P_o	peak energy wave period based on the observations, s.
P_m	peak energy wave period based on the wave model results, s.
P_{lb}	lower bound of P_o, s.
P_{ub}	upper bound of P_o, s.
Σ_{pr}	standard deviation of pressure, mm.
τ	bottom stress, Pascals.
τ_o	bottom stress derived from the observations, Pascals.
τ_m	bottom stress derived from the wave model results, Pascals.
τ_b	bottom stress required for bed load movement, Pascals.
τ_r	bottom stress required for resuspension, Pascals.

[32] **Acknowledgments.** The technical assistance of Ronald Muzzi (GLERL), Terry Miller (GLERL), and Robert White (ANL) in preparing and deploying the moorings is gratefully acknowledged. The captains and crews of the research vessels *Shenehon* (GLERL), *Neeskay* (University of Wis-

consin at Milwaukee), and *Lake Guardian* (U.S. Environmental Protection Agency) did their usual outstanding job in deploying and retrieving the moorings. Weiqi Lin and Larry Sanford generously provided the code used to recalculate the surface wave periods to account for the attenuation of the waves with depth. This project was supported by grants from the NOAA Coastal Ocean Program to B. M. Lesht and D. Schwab, and by internal GLERL funds for N. Hawley. The thoughtful comments by two anonymous reviewers are gratefully acknowledged. This is GLERL contribution 1268.

References

Beletsky, D., and D. J. Schwab (2001), Modeling circulation and thermal structure in Lake Michigan: Annual cycle and interannual variability, *J. Geophys. Res.*, *106*, 19,745–19,771.

Cahill, R. A. (1981), Geochemistry of recent Lake Michigan sediments, *Circ. 517*, 94 pp., Illinois State Geol. Surv., Champaign, Ill.

Hawley, N. (2000), Sediment resuspension near the Keewenaw Peninsula, Lake Superior, during the fall and winter, 1990–1991, *J. Great Lakes Res.*, *26*, 495–505.

Hawley, N., and C.-H. Lee (1999), Sediment resuspension and transport in Lake Michigan during the unstratified period, *Sedimentology*, *46*, 791–805.

Hawley, N., X. Wang, B. Brownawell, and R. Flood (1996), Resuspension of bottom sediments in Lake Ontario during the unstratified period, 1992–1993, *J. Great Lakes Res.*, *23*, 707–721.

Horikawa, K. (1988), *Nearshore Dynamics and Coastal Processes*, 522 pp., Univ. of Tokyo Press, Tokyo.

Lesht, B. M. (1989), Climatology of sediment transport on Indiana Shoals, Lake Michigan, *J. Great Lakes Res.*, *13*, 486–497.

Lesht, B. M., and N. Hawley (1987), Near-bottom currents and suspended sediment concentration in southeastern Lake Michigan, *J. Great Lakes Res.*, *13*, 375–386.

Lesht, B. M., and N. Hawley (2001), Using wave statistics to drive a simple sediment transport model, in *Ocean Wave Measurement and Analysis: Proceedings of the Fourth International Symposium Waves 2001*, pp. 1366–1375, Am. Soc. of Civ. Eng., Reston, Va.

Li, M. Z., and C. L. Amos (2001), SEDTRANS96: The upgraded and better calibrated sediment-transport model for continental shelves, *Comput. Geosci.*, *27*, 619–645.

Lick, W., J. Lick, and C. K. Ziegler (1994), The resuspension and transport of fine-grained sediments in Lake Erie, *J. Great Lakes Res.*, *20*, 599–613.

Lin, W., L. P. Sanford, B. J. Alleva, and D. J. Schwab (1997), Surface wind wave modeling in Chesapeake Bay, in *Ocean Wave Measurement and Analysis, Proceedings of the Conference*, pp. 1048–1062, Am. Soc. of Civ. Eng., Reston, Va.

Lin, W., L. P. Sanford, and S. E. Suttles (2002), Wave measurement and modeling in Chesapeake Bay, *Cont. Shelf Res.*, *22*, 2673–2686.

Liu, P. C., D. J. Schwab, and J. R. Bennett (1984), Comparison of a two-dimensional wave prediction model with synoptic measurements in Lake Michigan, *J. Phys. Oceanogr.*, *14*, 1514–1518.

Liu, P. C., D. J. Schwab, and R. E. Jensen (2002), Has wind-wave modeling reached its limit?, *Ocean Eng.*, *29*, 81–98.

Lou, J., D. J. Schwab, D. Beletsky, and N. Hawley (2000), A model of sediment resuspension and transport dynamics in southern Lake Michigan, *J. Geophys. Res.*, *105*, 6591–6610.

Panofsky, H. A., and G. W. Brier (1968), *Some Applications of Statistics to Meteorology*, 224 pp., Penn. State Univ. Press, University Park.

Sanford, L. P., and J. P.-Y. Maa (2001), A unified erosion formulation for fine sediments, *Mar. Geol.*, *179*, 9–23.

Schwab, D. J., and D. Beletsky (1998), Lake Michigan mass balance study: Hydrodynamic modeling project, *NOAA Tech. Memo. ERL GLERL-108*, 53 pp., Great Lakes Environ. Res. Lab., Ann Arbor, Mich.

Schwab, D. J., J. R. Bennet, and P. C. Liu (1984), Application of a simple numerical wave prediction model to Lake Erie, *J. Geophys. Res.*, *89*, 3586–3592.

Schwab, D. J., D. Beletsky, and J. Lou (2000), The 1998 coastal turbidity plume in Lake Michigan, *Estuarine Coastal Shelf Sci.*, *50*, 49–58.

N. Hawley and D. J. Schwab, Great Lakes Environmental Research Laboratory, 2205 Commonwealth Boulevard, Ann Arbor, MI 48105, USA. (nathan.hawley@noaa.gov; david.schwab@noaa.gov)

B. M. Lesht, Argonne National Laboratory, 9700 S. Cass Avenue, Argonne, IL 60439, USA. (bmlesht@anl.gov)